

The Relativistic Geoid: Gravity Potential and Relativistic Effects

Dennis Philipp,^{1,2} Eva Hackmann,¹ Claus Lämmerzahl,^{1,3,4} and Jürgen Müller^{5,6}

¹ZARM, University of Bremen, 28359 Bremen, Germany

²Fraunhofer MEVIS, 28359 Bremen, Germany

³DLR-Institute for Satellite Geodesy and Inertial Sensing,
c/o University of Bremen, Am Fallturm 2, 28359 Bremen, Germany

⁴Institute of Physics, Carl von Ossietzky University Oldenburg, 26111 Oldenburg, Germany

⁵IfE, University of Hannover, 30167 Hannover, Germany

⁶DLR-Institute for Satellite Geodesy and Inertial Sensing,
c/o Leibniz Universität Hannover, Welfengarten 1, 30167 Hannover, Germany

The Earth's geoid is one of the most important fundamental concepts to provide a gravity field-related height reference in geodesy and associated sciences. To keep up with the ever-increasing experimental capabilities and to consistently interpret high-precision measurements without any doubt, a relativistic treatment of geodetic notions (including the geoid) within Einstein's theory of General Relativity is inevitable. Building on the theoretical construction of isochronometric surfaces and the so-called redshift potential for clock comparison, we define a relativistic gravity potential as a generalization of known (post-)Newtonian notions. This potential exists for any stationary configuration and rigidly co-rotating observers. It is the same as realized by local plumb lines. In a second step, we employ the gravity potential to define the relativistic geoid in direct analogy to the Newtonian understanding. In the respective limits, it allows to recover well-known (post-)Newtonian results. For a better illustration and proper interpretation of the general relativistic gravity potential and geoid, we consider some particular examples. Explicit results are derived for exact vacuum solutions to Einstein's field equation as well as a parametrized post-Newtonian model. Comparing the Earth's Newtonian geoid to its relativistic generalization is a very subtle problem. However, an isometric embedding into Euclidean three-dimensional space can solve it and allows a genuinely intrinsic comparison. With this method, the leading-order differences are determined, which are at the mm-level.

PACS numbers: 91.10.-v, 04.20.-q, 91.10.By

I. INTRODUCTION

The ever-increasing technological capabilities allow to perform gravity and clock measurements with incredible accuracy. On the one hand, high-precision satellite missions such as GRACE/GRACE-FO allow to deduce properties of the Earth's gravity field, its changes on various time scales, and the investigation of underlying phenomena [1–3]. On the other hand, Earth-bound clock comparison networks or portable optical atomic clocks are used in the framework of chronometric geodesy [4–7]. One of the central notions that is to be determined by such geodetic measurements is the Earth's geoid - its mathematical figure as the German mathematician C.F. Gauss has termed it. Geoid determination with high accuracy is necessary for, e.g., national and global height systems and is related to various applications such as GNSS.

To thoroughly explain the outcome of contemporary and future geodetic missions at the cutting edge of available accuracy, we have to keep up at the theoretical level. Consequently, geodetic notions and concepts must be developed within a relativistic theory of gravity. The best available framework, consistent with all tests, is Einstein's theory [8]. Therefore, it is our goal to generalize known geodetic concepts and define all notions intrinsically within General Relativity.

In this work, we define a relativistic gravity potential,

which generalizes the Newtonian concept. It exists for any stationary configuration with observers on isometric congruences, i.e. observers who rigidly co-rotate with the Earth¹. Its definition is based on the philosophy of Bjerhammar [9, 10] and Soffel et al. [11] as well as results on the time-independent redshift potential in Ref. [12]. Our definition of the relativistic gravity potential allows to define and generalize geodetic notions such as the geoid in an intrinsic general relativistic manner. Moreover, it can be used to calculate the outcome of redshift and acceleration measurements, and it is realized by clock comparison as well as the determination of local plumb lines.

One significant result is the direct comparison of the conventional Newtonian geoid and its relativistic generalization. Such a comparison is of direct relevance for geodesy, but involves a lot of subtle points. In particular, there is some gauge freedom in the choice of constants, different applicable conventions, and the more crucial geometrical problem of comparing objects that live in different geometries.

The structure of this work is as follows. After introducing the relativistic gravity potential, we use it to give a definition of the relativistic geoid, and we show how the potential can be used to express clock comparison

¹ By configuration we mean a spacetime model for the Earth's exterior.

and acceleration measurements between observers on the Earth's surface. Our definition of the geoid is such that it is the surface which is locally orthogonal to plumb lines and coincides with the surface of vanishing mutual redshifts of standard clocks on Killing congruences. Therefore, different measurements can contribute to its realization in data fusion.

We apply our definitions to some particular spacetime examples for illustration of the concept and proper interpretation. A first-order parametrized post-Newtonian metric is employed to show that results in the literature are embedded into our framework. We also calculate exact expressions for the Schwarzschild spacetime, the quadrupolar Erez-Rosen spacetime, general asymptotically flat Weyl metrics, and the Kerr spacetime.

In the last part, we perform the comparison of the conventional Newtonian geoid and the relativistic generalization. Involved subtleties are overcome by an isometric embedding of the relativistic geoid surface into Euclidean three-dimensional space, and we show that the leading order difference, for a suitable convention, is about 2 mm due to the relativistic monopole. This embedding is not only an academic endeavor but necessary to overcome coordinate-dependent effects.

II. CONVENTIONAL UNDERSTANDING AND PREVIOUS RESULTS

In this section, we briefly summarize the conventional understanding of the geoid in Newtonian gravity as well as generalizations that exist so far within (approximate) relativistic frameworks. We start with the Newtonian geoid and consider the post-Newtonian extension thereafter. In addition, we summarize helpful references in geodetic and general relativistic literature.

A. Newtonian Geoid

In Newtonian gravity, the geoid is defined as one particular level surface of the gravity potential² [13]

$$W(\vec{X}) := U(\vec{X}) + V(\vec{X}), \quad (1)$$

where $U(\vec{X})$ is the Newtonian gravitational potential and $V(\vec{X})$ is the centrifugal potential experienced by rigidly co-rotating observers on the Earth's surface. We deliberately make the distinction between gravitation and gravity here to match geodetic notions and conventions. In Earth-centered global spherical coordinates (R, Θ, Φ) , we

then have for the centrifugal potential

$$V(\vec{X}) := -\frac{1}{2}\omega^2 d_z^2 = -\frac{1}{2}\omega^2 R^2 \sin^2 \Theta, \quad (2)$$

and the expansion of the gravitational potential into spherical harmonics reads

$$U(R, \Theta, \Phi) = -\frac{GM}{R} \sum_{l=0}^{\infty} \sum_{m=0}^l \left(\frac{R_{\text{ref}}}{R}\right)^l P_{lm}(\cos \Theta) \times [C_{lm} \cos(m\Phi) + S_{lm} \sin(m\Phi)]. \quad (3)$$

In the equations above, ω is the angular frequency of the Earth's rotation, R_{ref} is some chosen reference radius, and d_z is the distance to the rotation axis which points into the z -direction. The P_{lm} are the Legendre functions of degree l and order m , and C_{lm}, S_{lm} are multipole expansion coefficients. The gravitational potential is a solution of Poisson's equation (Laplace's equation outside the sources) and adapted to the condition that $U \rightarrow 0$ for $R \rightarrow \infty$. Note that in our sign convention the gravity potential is always negative since it refers to an attractive force. Under the assumption of axial symmetry, the expansion simplifies to

$$U(R, \Phi) = -\frac{GM}{R} \sum_{l=0}^{\infty} J_l \left(\frac{R_{\text{ref}}}{R}\right)^l P_l(\cos \Theta), \quad (4)$$

where the J_l are axially-symmetric multipole moments. A suitable definition of the Newtonian geoid now is the following.

Definition: The Earth's geoid is defined by the level surface of the gravity potential $W(\vec{X})$ such that

$$-W(\vec{X})|_{\text{geoid}} = W_0 = \text{constant}, \quad (5)$$

with a constant $W_0 = 6.263\,685\,34 \times 10^7 \text{ m}^2 \text{ s}^{-2}$, which complies with modern conventions [13, 14]. The numerical value of W_0 is chosen in a way to have the geoid coincide best with the mean sea level at rest and a history of measurements and previous conventions, see Ref. [14]. In contrast to usual geodetic formulations, we use a negative potential such that our convention in Eq. (5) differs by a sign. However, we want to keep the numerical value of W_0 to be strictly positive.

B. Post-Newtonian and Genuinely Relativistic Approaches

The first attempt to define a relativistic geoid was undertaken by Bjerhammar [9, 10] in 1985. He defined the geoid to be the surface on which "precise clocks run with the same speed". Inspired by Bjerhammar's approach, which, however, lacks some formal and mathematical clarity, we give a relativistic geoid definition based on clock comparison. The essential steps to do so have already been outlined in Refs. [12, 15, 16], in which the

² Note that in conventional geodesy, the gravitational potential is usually denoted by V whereas the centrifugal potential is denoted by Z .

relativistic geoid is defined in terms of isochronometric surfaces, the level sets of a so-called stationary redshift potential for Killing congruences. We will, to a large extent, use the results in these references and incorporate them into the definition of a relativistic gravity potential in the next section.

Several authors also investigated the Earth’s geoid in a post-Newtonian framework; see, e.g., Refs. [11, 17–19]. The principle idea is to use potentials defined at the order of $1/c^2$ in a first-order post-Newtonian approximation of General Relativity. The relativistic geoid can then be defined by a special level surface again but is valid to first order only. In this context, the notions of the u-geoid and a-geoid appear, related to definitions in terms of clocks and their comparison on the one hand and accelerations of observers on the other hand, see Ref. [11]. However, the choice of a particular surface w.r.t. the Newtonian limit as well as an intrinsic relativistic understanding is generally not elaborated. Concerning a general relativistic definition, the work in Ref. [20] must be mentioned, in which the authors define the geoid in terms of quasi-local frames. Furthermore, in Ref. [19], an exact definition of the geoid and a generalization of the disturbing potential in General Relativity are analyzed via perturbations of a chosen background manifold.

For the geodetic community also the difference between Newtonian and generalized notions is of great interest. As we will show in the next sections, in such a comparison some subtle details are involved, but they can be handled genuinely within a general relativistic framework without approximations. Thus, intrinsic geometric properties are conserved and not spoiled by an approximative description.

III. RELATIVISTIC GRAVITY POTENTIAL AND THE GEOID

To arrive at an intrinsic relativistic understanding of a stationary object’s geoid, we build on some of the ideas in Refs. [11, 19] together with our previous results in Ref. [12]. Thereupon, we present a framework that is consistent within General Relativity without any approximation and allows to recover previously known (post-) Newtonian results in the respective limits.

The next section contains a summary of significant results regarding clock comparison, isometric observer congruences, the mutual redshift of standard clocks, and isochronometric surfaces. Thereupon, we define a relativistic gravity potential that is, in turn, used to define the relativistic geoid in analogy to the Newtonian understanding.

We use SI-units to explicitly see where the speed of light c and Newton’s gravitational constant G enter into the formulae. Greek indices are spacetime indices and shall range from 0 to 3, whereas Latin indices are purely spatial indices, and they take values from 1 to 3.

A. Observer Congruence and Redshift Potential

Any stationary metric can be written in the form

$$g = e^{2\phi(x)} [-(c dt + \alpha_a(x) dx^a)^2 + \alpha_{ab}(x) dx^a dx^b], \quad (6)$$

in which the coordinates $(x^0 = ct, x^i)$ for $i = 1 : 3$ are assumed to be co-rotating and are adapted to the symmetry. Let us assume that Eq. (6) describes the exterior of some astronomical object of interest. Given the geodesy of our planet, we use this metric to build a model of the Earth’s exterior spacetime. Because of the lack of better wording, we will also speak of the geodesy of other objects and define the geoid in a way that works generally. Now, we think of observers that rigidly co-rotate with the object of interest³. They transport standard clocks with them and parametrize their respective worldlines by their individual proper time. Since the coordinates are co-rotating, these observers are hovering on fixed positions ($dx^i = 0$) or might be attached to the surface if there is any. Such observers are described by integral curves of the vector field $\xi_{(1)} := \partial_t$. For the Earth, this means we consider in particular observers (measurement stations equipped with atomic clocks and gravimeters) attached to its physical surface. The worldlines of these observers form an isometric (Killing) congruence, and there are some important conclusions. As shown in Ref. [12], for a spacetime with a metric in the form of (6) there exists a time-independent redshift potential. It describes the relative frequency difference between any two standard clocks on worldlines in the congruence. This redshift potential is given by the scalar function $\phi(x)$ and two observers on worldlines γ_1 and γ_2 , respectively, determine their mutual redshift

$$1 + z := \frac{\nu_1}{\nu_2} = \exp(\phi|_{\gamma_2} - \phi|_{\gamma_1}) =: \exp(\Delta\phi), \quad (7)$$

in which $\nu_{1,2}$ is the frequency of an exchanged light signal as seen by the respective observer. The redshift potential and the redshift are dimensionless.

As shown in Ref. [12], a definition of the relativistic geoid can be given in terms the redshift potential’s level sets. These equipotential surfaces are called isochronometric, i.e. two standard clocks on the same level surface have a vanishing mutual redshift. Therefore, the relativistic geoid is defined in Bjerhammar’s philosophy as “the surface on which all clocks run with the same speed” but with more mathematical rigour and intrinsic general relativistic notions. We want to point out here, that this definition remains valid in the following, but we will use new notions to make it accessible and also more intuitive with clear non-relativistic limits. Moreover, the definition will enable a direct comparison to existing post-Newtonian results and shed some light on the order of magnitude of deviations from the conventional geoid.

³ Alternatively, also the constituents of the Earth in a rigid model follow the same worldlines.

B. Gravity Potential

We assume that Einstein's field equation is fulfilled and the configuration is asymptotically flat and stationary. Given a relativistic spacetime model of the Earth with a metric (6) that allows for the existence of a time-independent redshift potential ϕ for observers who are rigidly co-rotating, i.e. observers who form an isometric congruence, we construct the following.

Definition: Let the relativistic gravity potential U^* be defined by the following relation to the observers' time-independent redshift potential ϕ [16]:

$$e^\phi =: 1 + \frac{U^*}{c^2} \Leftrightarrow U^* = c^2 (e^\phi - 1) = c^2 (\sqrt{-g_{00}} - 1), \quad (8)$$

where we use co-rotating coordinates as defined above. The dimension of U^* is the square of a velocity, $[U^*] = [c^2] = \text{m}^2/\text{s}^2$. The intention of defining the new potential U^* as done above becomes evident in the Newtonian limit, in which our relativistic gravity potential U^* becomes the Newtonian gravity potential W , i.e.

$$U^* \xrightarrow{c \rightarrow \infty} W. \quad (9)$$

This is easily verified by expanding the square root in Eq. (8) in the usual way, assuming a weak field limit exists. Centrifugal effects are included since the coordinates are adapted to a rigidly co-rotating congruence of observers such that they move on integral curves of the Killing vector field $\xi_{(1)} = \partial_t$. Note in particular that in our sign convention also $U^* < 0$ everywhere. Hence, it has the same sign as Newton's gravity potential W . A definition of the relativistic geoid in terms of U^* will then also resemble the conventional Newtonian definition in terms of W in the limit.

C. Redshift and Acceleration

Using the potential U^* we can express redshift relations and acceleration measurements for worldlines in the congruence of observers in the following way.

a) Redshift of two rigidly co-rotating observers

Let the worldlines of two observers in the congruence be γ_1 and γ_2 , respectively, and assume they measure their respective proper time, i.e. they are equipped with standard clocks. We evaluate the redshift potential ϕ and the relativistic gravity potential U^* on their respective worldlines to have values

$$\phi_i := \phi|_{\gamma_i} \quad \text{and} \quad U_i^* := U^*|_{\gamma_i} \quad i = 1, 2. \quad (10)$$

The frequency ratio of their standard clocks is then given by

$$\begin{aligned} 1 + z &:= \frac{\nu_1}{\nu_2} = e^{\phi_2 - \phi_1} = \frac{1 + U_2^*/c^2}{1 + U_1^*/c^2} \\ &= 1 + \frac{U_2^* - U_1^*}{c^2} + \mathcal{O}(c^4) =: 1 + \frac{\Delta U^*}{c^2} + \mathcal{O}(c^4). \end{aligned} \quad (11)$$

Hence, the relativistic gravity potential U^* determines the redshift. To leading order, the redshift is given by the potential differences, and it vanishes in the Newtonian limit since Newton's universal time is absolute. But to first post-Newtonian order we obtain as the largest contribution

$$\frac{\nu_1}{\nu_2} = 1 + \frac{\Delta W}{c^2} + \mathcal{O}(c^{-3}), \quad (12)$$

since U^* can be expressed as

$$U^* = W + \sum_{n=2} \Xi_n/c^n, \quad (13)$$

where the Ξ_n are post-Newtonian correction terms of order n .

Note, however, that our definition of U^* is exact, i.e. without any approximation, and it is valid for an arbitrary stationary spacetime with a metric as given above. Thus, we have constructed an intrinsic general relativistic analog of the concepts introduced by Soffel *et al.* in Ref. [11]. In this work, the authors derive a similar expression but work within a first-order post-Newtonian approximation only.

b) Acceleration of freely falling objects w.r.t. rigidly co-rotating observers

Using the fact that the acceleration potential of an isometric congruence is the same as its redshift potential, see Ref. [12], we can express the acceleration of freely falling test masses w.r.t. the congruence in terms of U^* ,

$$a = -c^2 d\phi = -c^2 \frac{\partial \phi}{\partial U^*} dU^* = \frac{-dU^*}{1 + U^*/c^2}. \quad (14)$$

Here, d denotes the exterior derivative. The one form acceleration a is closed and exact. Its components can be calculated by $a_\mu = -c^2 \partial_\mu \phi$ and it is clear that $a_0 \equiv 0$. Thus, $(a_\mu) = (0, a_1, a_2, a_3)$ and the components are

$$a_i = -c^2 \partial_i \phi = -c^2 e^{-\phi} \partial_i e^\phi = \frac{-\partial_i U^*}{1 + U^*/c^2}. \quad (15)$$

We notice that U^* , or rather its scaled gradient, determines the acceleration of freely falling test masses. The level surfaces $\phi = \text{const.}$, i.e. $U^* = \text{const.}$, are everywhere perpendicular to the acceleration - that is perpendicular to the local plumb lines.

In the weak-field limit we also recover the well known Newtonian formula⁴

$$\vec{g} = -\vec{\nabla}W, \quad (16)$$

according to which the gravity vector is determined by the gradient of the gravity potential. For the magnitude of the relativistic acceleration we obtain

$$\frac{a^2}{c^4} = \frac{g(a, a)}{c^4} = g^{ij} \partial_i \phi \partial_j \phi \quad (17a)$$

$$\Rightarrow a^2 = g^{ij} \frac{\partial_i U^* \partial_j U^*}{(1 + U^*/c^2)^2}, \quad (17b)$$

from which the usual Newtonian definition of scalar gravity follows in the weak field limit⁵,

$$g^2 = (\vec{\nabla}W)^2 \Leftrightarrow g = \|\vec{\nabla}W\|_2, \quad (18)$$

in which $\|\cdot\|_2$ is the Euclidean norm.

D. The Relativistic Geoid

Definition: For a spacetime equipped with a metric of the form

$$g = \left(1 + \frac{U^*}{c^2}\right)^2 \left[-(cdt + \alpha_a(x)dx^a)^2 + \alpha_{ab}(x)dx^a dx^b\right] \quad (19)$$

and a congruence of rigidly co-rotating observers who move on integral curves of the Killing vector field $\xi_{(1)} = \partial_t$, the relativistic geoid is a particularly chosen level surface of the relativistic gravity potential U^* such that

$$U^*|_{\text{geoid}} = U_0^* = \text{const}. \quad (20)$$

Level surfaces of U^* are level surfaces of ϕ , and therefore, they are isochronometric. The observers' worldlines are integral curves of the vector field $u = (1 + U^*/c^2)^{-1} \xi_{(1)}$. Consequently, in a stationary general relativistic model for the exterior of the Earth, the relativistic geoid, as determined by either clock comparison or plumb line directions, is given by the particular two-dimensional isochronometric surface on which Eq. (20) holds.

The Newtonian limit of our relativistic definition is apparent. Because the weak field limit of U^* is W , the Newtonian definition in terms of level surfaces of the gravity potential W , such that on the geoid $W = -W_0$, is recovered. The value U_0^* , which singles out one such equipotential surface to be the relativistic geoid, must be given by some convention which is agreed upon. Two possibilities are, e.g.,

(i) to fix the value by the conventional Newtonian gravity potential on the geoid such that $U_0^* \equiv -W_0$,

(ii) to define a master clock which is, by definition, situated on the geoid's surface and singles out one isochronometric surface in a geometrical way (e.g., the one that passes through its center of mass). Then, U_0^* is related to the work done to bring a unit mass from infinity to the clock's position.

Note that the choice (ii) is equivalent to marking a point (possibly at the shore), representing the mean sea level, and therefore choosing a level surface for U^* in a geometric manner. Also the construction of a so-called clock compass [21] might be employed to fix a particular isochronometric surface and to test all clocks w.r.t. it.

Our definition in terms of the relativistic gravity potential is exact and it does not only apply to the Earth but also to arbitrarily compact objects as long as the requirements listed above are fulfilled. The definition of the geoid in various exact spacetimes⁶ can now be calculated by expressing their respective metric in the form (6) and reading off the relativistic gravity potential. In this way, also a comparison to results in an approximative post-Newtonian framework is possible. The results are presented in the next section.

E. Examples and Limits

In this section we show particular examples for the application of our definition. We consider a first-order parametrized post-Newtonian framework, general Weyl solutions that include in particular the Schwarzschild and Erez-Rosen spacetime, and the Kerr metric that exhibits gravitomagnetic effects. We argue that exact spacetimes play a useful role in relativistic geodesy and should be employed to explicitly define, understand, and calculate conceptual notions and quantities, c.f. Ref. [22].

1. Parametrized post-Newtonian Framework

In harmonic co-rotating coordinates ($x^0 = ct, x, y, z$), the metric components for the parametrized post-Newtonian spacetime that describes the Earth's exterior

⁴ Note that in this limit the indices are raised and lowered with the Kronecker delta δ_{μ}^{ν} .

⁵ In all the equations above, $\vec{\nabla}$ is the flat space operator.

⁶ By exact spacetimes we understand exact solutions of Einstein's field equation.

can be given by ⁷

$$g_{00}(\mathbf{x}) = - \left(1 + \frac{2W(\mathbf{x})}{c^2} + \frac{2\beta U(\mathbf{x})^2}{c^4} \right) + \mathcal{O}(c^{-6}), \quad (21a)$$

$$g_{0i}(\mathbf{x}) = - \frac{2(\gamma + 1) |U^i(\mathbf{x})|}{c^3} - \frac{\epsilon_{ijk} x^j \omega^k}{c} + \mathcal{O}(c^{-5}), \quad (21b)$$

$$g_{ij}(\mathbf{x}) = \delta_{ij} \left(1 - \frac{2\gamma U(\mathbf{x})}{c^2} \right) + \mathcal{O}(c^{-4}), \quad (21c)$$

see, e.g., Refs. [8, 23, 24]. Here, $\vec{\omega}$ is the Earth's rotation vector pointing in the x^3 -direction and U^i is the post-Newtonian vector potential [8, 25]. In these coordinates, rigidly co-rotating observers on the Earth's surface are described by $dx^i = 0$. Note that we can express $g_{0i}(\mathbf{x})$ also in the form

$$g_{0i}(\mathbf{x}) = - \frac{\gamma + 1}{c^3} L_i - \frac{\epsilon_{ijk} x^j \omega^k}{c}, \quad (22)$$

with the Earth's gravitomagnetic field [11, 26]

$$\vec{L}_\oplus = \frac{G \vec{J}_\oplus \times \vec{x}}{R^3}, \quad (23)$$

and the total angular momentum \vec{J}_\oplus of the Earth. For a spherical central mass M with radius R_0 , rotating around the x^3 -axis with angular velocity ω , the gravitomagnetic vector potential can be evaluated easily and we obtain

$$g_{03} = - \frac{2(\gamma + 1) GM/R}{5c^3} \left(\frac{R_0}{R} \right)^2. \quad (24)$$

The post-Newtonian approximation of General Relativity is obtained for $\beta = 1$ and $\gamma = 1$.

With the definition (8), the relativistic gravity potential U_{ppN}^* for the parametrized post-Newtonian metric is

$$U_{\text{ppN}}^* = W + \frac{U^2(\beta - 1/2)}{c^2}, \quad (25)$$

and for the post-Newtonian approximation of General Relativity we get

$$U_{\text{pN}}^* = W + \frac{U^2}{2c^2}. \quad (26)$$

Hence, deviations from the Newtonian gravity potential are described by the second term in (25) which is proportional to U^2/c^2 . Note that this result coincides with the findings in Refs. [11, 19]. However, the relativistic gravity potential U^* here is defined without any approximations regarding the strength of the gravitational field, in contrast to the authors' results. Thus, we have shown

that our framework also covers well-known notions in an appropriately constructed limit of General Relativity.

Let us assume that we send signals from one observer on the worldline γ_1 to another observers on the worldline γ_2 , and both observers rigidly co-rotate with the Earth. To the appropriate order $\mathcal{O}(c^{-2})$, the redshift of the signal as determined by standard clocks is

$$1 + z = \frac{\nu_1}{\nu_2} = \frac{1 + U_2^*/c^2}{1 + U_1^*/c^2} = 1 + \frac{W_2 - W_1}{c^2} + \mathcal{O}(c^{-4}), \quad (27)$$

where $U_i^* := U^*|_{\gamma_i}$ and $W_i := W|_{\gamma_i}$ for $i = 1, 2$. We observe that to first-order in the parametrized post-Newtonian framework the redshift is proportional to $\Delta W := W_2 - W_1$ and it is not sensitive to the ppN parameters β and γ . In fact, with (27) we have just derived the fundamental equation of chronometric geodesy. However, since we derived it in a top-down approach, we know how it is conceptually embedded in a broader theoretical framework; this gives some trust in its validity and it is not only an approximative result which could, in principle, become useless at the full theoretical level.

The leading order contribution to the redshift is due to the relativistic monopole moment and given by the redshift result for the Schwarzschild spacetime, see below. Close to the Earth's surface, we find the correspondence between a height difference of two clocks and the redshift signal. The redshift is roughly 10^{-16} per meter height distance. For most applications related to clock comparison close to the Earth's surface it will be sufficient to expand the gravity potential in Eq. (27) up to multipolar order proportional to J_2 in Eq. (4). For a small spatial distance between the two clocks, the expansion of the gravity potential W_2 around the value W_1 leads to

$$W_2 = W_1 + \vec{\nabla} W \cdot (\vec{X}_2 - \vec{X}_1) + \mathcal{O}(|\vec{X}_2 - \vec{X}_1|^2). \quad (28)$$

Hence, we obtain

$$W_2 = W_1 - \bar{g}_{12} H_{12} + \mathcal{O}(H_{12}^2), \quad (29)$$

in terms of the orthometric height H_{12} [13] between both clock positions. Here, \bar{g}_{12} denotes the averaged gravity between the clocks' positions along the plumb line. Therefore, the redshift becomes

$$z(H_{12}) \approx \bar{g}_{12} \frac{H_{12}}{c^2}. \quad (30)$$

Hence, redshift measurements are useful to determine the orthometric height, provided that they are supported by gravity measurements. Indeed, geodetic leveling measurements must always be supported by matching gravity observations to conclude meaningful height measures.

The relativistic geoid in the parametrized post-Newtonian spacetime is given by one particular isochronometric surface, which is an equipotential sur-

⁷ We use only the parameters β and γ here.

face of U_{ppN}^* such that

$$U_{\text{ppN}}^* \Big|_{\text{geoid}} = W + \frac{U^2(\beta - 1/2)}{c^2} \Big|_{\text{geoid}} = U_0^* = \text{const.} \quad (31)$$

For the post-Newtonian approximation of General Relativity we obtain

$$U_{\text{pN}}^* \Big|_{\text{geoid}} = W + \frac{U^2}{2c^2} \Big|_{\text{geoid}} = U_0^* = \text{const.} \quad (32)$$

Thus, high-accuracy geoid determination might give bounds on the value of β . The result above will be used later to access the leading-order relativistic corrections to the Newtonian geoid. Our results here are consistent with the literature, see Ref. [11].

We now calculate the covariant acceleration components a_i , the contravariant components a^i , and the norm of the acceleration a at the level of $\mathcal{O}(1/c^2)$ accuracy:⁸

$$a_{i,\text{ppN}} = -\partial_i \left(W + \frac{U^2(\beta - 1)}{c^2} \right), \quad (33a)$$

$$a_{\text{ppN}}^i = -\delta^{ij} \partial_j \left(W + \frac{U^2(\beta + \gamma - 1)}{c^2} \right), \quad (33b)$$

which is equivalent to

$$\vec{a}_{\text{ppN}} = -\vec{\nabla} \left(W + \frac{U^2(\beta + \gamma - 1)}{c^2} \right) =: -\vec{\nabla} \bar{U}_{\text{ppN}} \quad (33c)$$

$$a_{\text{ppN}} = \left\| \vec{\nabla} \left(W + \frac{U^2(\beta + \gamma/2 - 1)}{c^2} \right) \right\|_2 =: \|\vec{\nabla} \tilde{U}_{\text{ppN}}\|_2. \quad (33d)$$

Here, $\vec{\nabla}$ is the flat space operator such that $\|\vec{\nabla} \tilde{U}\|_2 = \sqrt{\delta^{ij} \partial_i \tilde{U} \partial_j \tilde{U}}$ in Cartesian coordinates.

As shown above in Eq. (33), we define two new potentials: (i) the potential \bar{U}_{ppN} , which determines the ‘‘acceleration vector’’ \vec{a}_{ppN} , and (ii) the potential \tilde{U}_{ppN} of which the norm of the gradient gives the scalar acceleration a_{ppN} . The results coincide with those in Ref. [11].

Note that for the parameter values of General Relativity ($\beta = 1, \gamma = 1$), we have

$$\bar{U}_{\text{pN}} = W + \frac{U^2}{c^2}, \quad (34a)$$

$$\tilde{U}_{\text{pN}} = U_{\text{pN}}^* = W + \frac{U^2}{2c^2}. \quad (34b)$$

Interestingly, for the post-Newtonian approximation of General Relativity it is true that $\tilde{U}_{\text{pN}} \equiv U_{\text{pN}}^*$, the relativistic gravity potential and the potential of which the

norm determines the magnitude of the acceleration coincide. However, measuring the acceleration of co-rotating observers on the Earth’s surface yields bounds on the value of the combination $(\beta + \gamma/2 - 1)$.

In this section, we have recovered and generalized the results of Ref. [11] which was one of the major sources of inspiration for the development of our framework that allows to develop all notions without any approximation. We regard it as a good test for our definitions that we successfully recover these results - be reminded of our sign convention for the comparison.

2. Weyl Metrics

In the following, we apply our framework to Weyl metrics, which are axisymmetric and static solutions to Einstein’s vacuum field equation⁹. We explicitly consider solutions which are asymptotically and elementary flat, see Ref. [27]. Special examples of this class of spacetimes are the Schwarzschild solution and the quadrupolar spacetime found by Erez and Rosen [28]. However, a straightforward generalization to higher order multipole spacetimes exists.

Written in spheroidal non-rotating coordinates (t, x, y, φ) , the Weyl metrics of interest read

$$g_{\mu\nu} dx^\mu dx^\nu = -e^{2\psi} c^2 dt^2 + m^2 e^{-2\psi} (x^2 - 1)(1 - y^2) d\varphi^2 + m^2 e^{-2\psi} e^{2\gamma} (x^2 - y^2) \left(\frac{dx^2}{x^2 - 1} + \frac{dy^2}{1 - y^2} \right). \quad (35)$$

The metric functions ψ, γ depend only on x and y , and m is a length parameter determined by the total mass. Einstein’s vacuum field equation for the metric above can be found, e.g., in Refs. [27] and [29]. In Ref. [27], Quevedo has shown that the general asymptotically flat solution with elementary flatness on the axis for the primary metric function is given by

$$\psi = \sum_{l=0}^{\infty} (-1)^{l+1} q_l Q_l(x) P_l(y). \quad (36)$$

Here, the Q_l are Legendre functions of the second kind, see the appendix and Ref. [30] for details. We call the expansion coefficients q_l Quevedo moments and they are related to Weyl’s moments for the expansion in his canonical coordinates. There is a clear relation to invariantly defined multipole moments¹⁰ and the Newtonian moments J_l in the weak field limit of a given Weyl spacetime. We have

$$J_l = (-1)^l \frac{l!}{(2l+1)!!} \left(\frac{m}{R_{\text{ref}}} \right)^l q_l, \quad (37)$$

⁸ Formally, the contravariant acceleration components can include a non-zero a^0 . However, we have $a_{\text{ppN}}^0 = 0 + \mathcal{O}(c^{-3})$.

⁹ Here, Weyl spacetimes mean solutions of Einstein’s field equation and we do not consider the context of Weyl’s theory of Gravitation.

¹⁰ We refer to the definition given by Geroch and Hansen [31, 32].

such that m is the mass monopole in geometric units and R_{ref} is a reference radius, see Eq. (4).

We now change to rotating coordinates to cover centrifugal effects and then we read off the relativistic gravity potential from the final form of the metric. This procedure allows to include inertial effects but of course fails to cover gravitomagnetic contributions since we still have a static spacetime at hand. From the metric (35) we conclude that two Killing vector fields $\xi_{(1)} = \partial_t$ and $\xi_{(2)} = \partial_\varphi$ exist, the latter of which is spacelike. Rigidly co-rotating observers move on integral curves of $\xi_{(1)} + \omega\xi_{(2)}$, in which ω is the angular velocity of rotation around the symmetry axis. For bounded values of ω the combination remains timelike. After coordinate transformation, we obtain the redshift potential

$$e^{\phi(x,y)} = \sqrt{e^{2\psi(x,y)} - \frac{\omega^2}{c^2} m^2 (x^2 - 1)(1 - y^2) e^{-2\psi(x,y)}}. \quad (38)$$

Note how Weyl's first metric function ψ enters the result. Now, we can insert the exact result¹¹

$$2\psi(x, y) = \sum_{l=0}^n (-1)^{l+1} q_l P_l(y) \times \left(\log \left(\frac{x+1}{x-1} \right) P_l(x) - 2 \sum_{k=0}^{[l/2-1/2]} \frac{2l-4k-1}{(l-k)(2k+1)} P_{l-2k-1}(x) \right), \quad (39)$$

which allows to evaluate the redshift potential at any multipolar level. The very first term proportional to q_0 reveals the Schwarzschild result and m is the Schwarzschild mass related to the radius $r_s = 2m$ for the choice $q_0 = 1$. To transform the result to usual area coordinates, the relation $x = r/m - 1$ must be used. Including also the next higher order term proportional to q_2 gives the redshift potential in the Erez-Rosen spacetime¹². Axisymmetric exact spacetimes with well-defined Newtonian limits can be constructed by including also q_n for $n > 2$, see Fig. 1 for a schematic overview. The relativistic gravity potential for such Weyl spacetimes is a rather lengthy expression. However, it can be calculated without any approximation and is of the form

$$U_{\text{Weyl}}^* = U_{\text{Weyl}}^*(\psi(x, y), x, y, m, q_l, \omega). \quad (40)$$

The surfaces $U^* = \text{const.}$ are isochronometric and for a given set of parameters one of them is the geoid after a suitable choice of a constant U_0^* . In the following we

give the explicit expressions for the Schwarzschild and Erez-Rosen spacetime, respectively.

The redshift potential for rigidly co-rotating observers in the Schwarzschild spacetime is

$$e^{\phi(r,\vartheta)} = \sqrt{-(g_{00}(r, \vartheta) + \omega^2 g_{\varphi\varphi}(r, \vartheta)/c^2)} \\ = \sqrt{1 - \frac{2m}{r} - \frac{\omega^2}{c^2} r^2 \sin^2 \vartheta}, \quad (41)$$

where we use standard area coordinates. The relativistic gravity potential for the Schwarzschild spacetime becomes

$$U_{\text{Schwarzschild}}^* = c^2 \left(\sqrt{1 - \frac{2GM}{c^2 r} - \frac{\omega^2}{c^2} r^2 \sin^2 \vartheta} - 1 \right). \quad (42)$$

Hence, the redshift between two members of the congruence at positions (r_1, ϑ_1) and (r_2, ϑ_2) , respectively, is

$$z + 1 = \frac{\nu_1}{\nu_2} = \frac{\sqrt{1 - \frac{2m}{r_2} - \frac{\omega^2}{c^2} r_2^2 \sin^2 \vartheta_2}}{\sqrt{1 - \frac{2m}{r_1} - \frac{\omega^2}{c^2} r_1^2 \sin^2 \vartheta_1}}, \quad (43)$$

and we find that close to the Earth's surface the redshift is about 10^{-18} per cm height difference. For the magnitude of the acceleration along the congruence we find

$$a = e^{-2\phi_2} \left(\left(1 - \frac{2GM}{c^2 r} \right) \left(\frac{GM}{r^2} - \omega^2 r \sin^2 \vartheta \right)^2 + \frac{1}{r^2} (\omega^2 r^2 \sin \vartheta \cos \vartheta)^2 \right)^{1/2}. \quad (44)$$

In the Newtonian limit, this becomes

$$g = \|\vec{\nabla} W\|_2, \quad W = -\frac{GM}{R} - \frac{1}{2} \omega^2 R^2 \sin^2 \Theta, \quad (45)$$

which is the gravity magnitude in a spherically symmetric field.

The Erez-Rosen spacetime can be used to describe the spacetime outside a quadrupolar Earth. It is a natural relativistic generalization of a quadrupolar Newtonian gravitational potential

$$U(R, \Theta) = -\frac{GM}{R} \left(1 + \frac{J_2 R_{\text{ref}}^2}{2R^2} (3 \cos^2 \Theta - 1) \right). \quad (46)$$

This particular Newtonian potential will be recovered in the weak-field limit of the Erez-Rosen spacetime. We can choose the parameters m and q_2 to let the relativistic monopole \mathcal{M}_0 and the quadrupole \mathcal{M}_2 coincide with the respective Newtonian moments of the Earth. To do so, we have to choose $m_\oplus = GM/c^2$ and q_2 must be

$$q_2 = \frac{15}{2} \left(\frac{R_{\text{ref}}}{m} \right)^2 J_2. \quad (47)$$

¹¹ The upper limit of summation $[l/2 - 1/2]$ denotes the closest integer smaller than the value of the expression in brackets.

¹² There is no relevant q_1 contribution since a dipole moment can always be made to vanish by a suitable coordinate transformation.

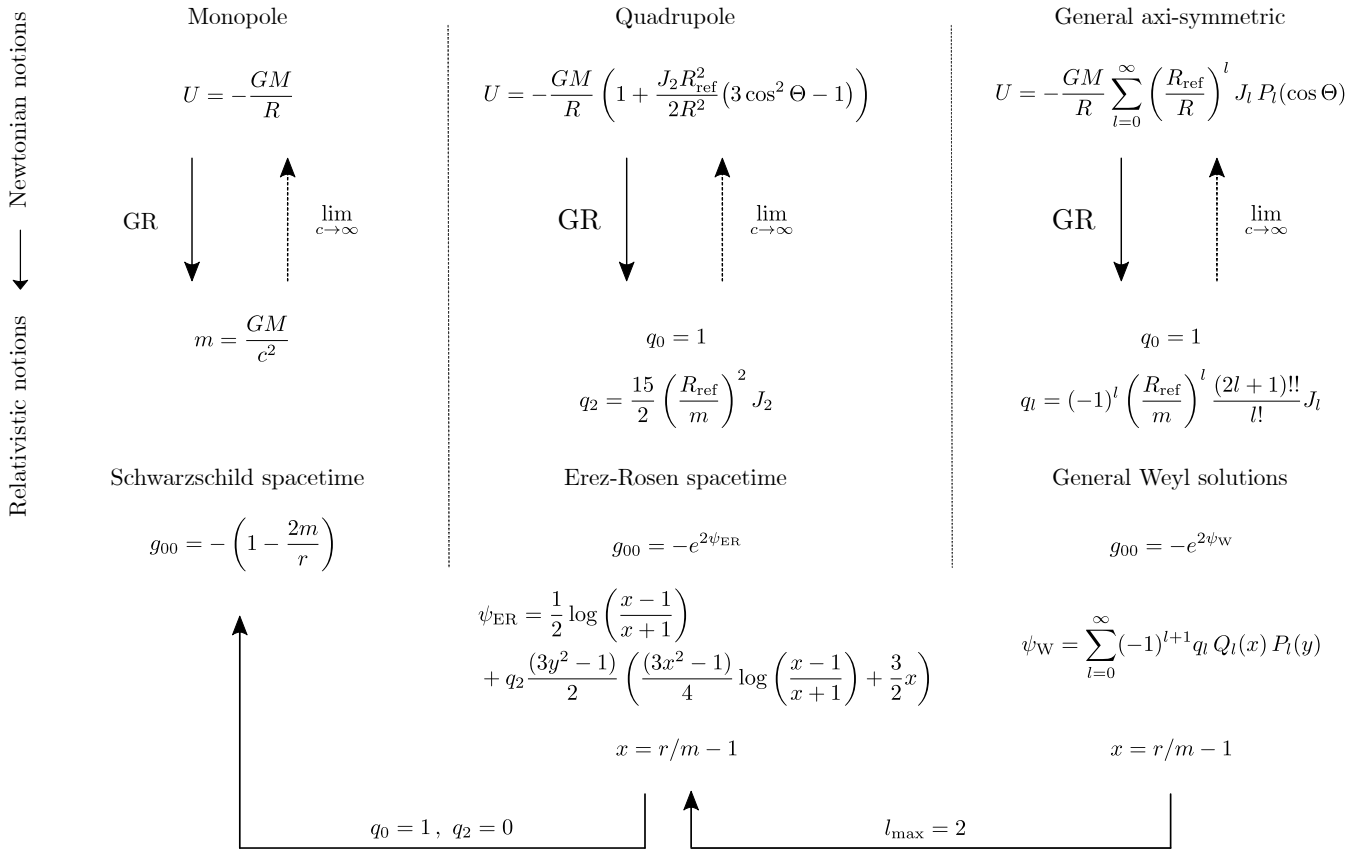


FIG. 1. An overview of the relation between Weyl solutions and the Erez-Rosen as well as the Schwarzschild metric as generalizations of Newtonian configurations. An axisymmetric Newtonian gravitational field is generalized by a general Weyl solution with parameters q_n . For $n_{\text{max}} = 2$, the Erez-Rosen spacetime is recovered as the generalization of a Newtonian quadrupolar model. If also $q_2 = 0$, we obtain the Schwarzschild solution as the relativistic monopole analog.

The redshift potential for rigidly co-rotating observers reads

$$e^{\phi(x,y)} = \sqrt{e^{2\psi_{\text{ER}}(x,y)} - \frac{\omega^2}{c^2} (GM/c)^2 (x^2 - 1)(1 - y^2) e^{-2\psi_{\text{ER}}(x,y)}}, \quad (48)$$

in which the metric function ψ_{ER} is given by

$$\psi_{\text{ER}(x,y)} = \frac{1}{2} \log\left(\frac{x-1}{x+1}\right) + q_2 \frac{(3y^2-1)}{2} \left(\frac{(3x^2-1)}{4} \log\left(\frac{x-1}{x+1}\right) + \frac{3}{2}x\right). \quad (49)$$

Using the expressions above, the relativistic gravity potential $U^*(\psi_{\text{ER}}(x,y), x, y, M, q_2, \omega)$ for the Erez-Rosen spacetime can be calculated analytically and the geoid is defined by a level surface in some chosen convention for U_0^* .

3. Kerr Spacetime

To investigate the influence of gravitomagnetic contributions, we apply our framework to the Kerr spacetime. In the standard Boyer-Lindquist coordinates, the metric is given by

$$g = -\left(1 - \frac{2mr}{\rho^2}\right) c^2 dt^2 + \frac{\rho^2}{\Delta} dr^2 + \rho^2 d\vartheta^2 + \sin^2 \vartheta \left(r^2 + a^2 + \frac{2mra^2 \sin^2 \vartheta}{\rho^2}\right) d\varphi^2 - \frac{4mra \sin^2 \vartheta}{\rho^2} c dt d\varphi, \quad (50)$$

and we introduce the abbreviations

$$\rho^2 = r^2 + a^2 \cos^2 \vartheta, \quad \Delta = r^2 + a^2 - 2mr. \quad (51)$$

The gravitomagnetic field of the Kerr spacetime approximates frame dragging effects in the Earth's vicinity very well, if parameters are chosen appropriately. The first

multipole moments of the Kerr metric are

$$\text{Mass monopole} \quad \mathcal{M}_0 = m, \quad (52a)$$

$$\text{Spin dipole} \quad \mathcal{S}_1 = ma, \quad (52b)$$

$$\text{Mass quadrupole} \quad \mathcal{M}_2 = -ma^2. \quad (52c)$$

The Kerr parameter is related to the angular momentum by $a = J/(Mc)$. Hence, we can choose m such that the Kerr monopole is the total mass of the Earth, and a such that the spin dipole is related to the Earth's angular momentum. To have this correspondence, we set $m_\oplus = GM/c^2$, as before. For a we use the relation of the angular momentum to the moment of inertia I , $J = I\omega$. For a rigidly rotating sphere with radius r_\oplus , we have $I = 2/5Mr_\oplus^2$. Hence, the Kerr parameter for the Earth becomes

$$a_\oplus = \frac{2}{5} \frac{\omega}{c} r_\oplus^2. \quad (53)$$

Calculating the values, we obtain $m_\oplus \approx 0.0044$ m and $a_\oplus \approx 892 m_\oplus$, where the radius and angular velocity as given by the EGM96 model are used [33]¹³. However, we have to state that the Kerr spacetime is also not a good approximation for the Earth's exterior in the sense that it covers gravitomagnetic effects but fails to represent the Earth's flattening and quadrupolar contribution at the right magnitude. Choosing the values for the mass monopole and the spin-dipole fixes the mass quadrupole uniquely. Therefore, we can not expect the Kerr spacetime to represent features of the flattened Earth.

We change again to rotating coordinates to find the relativistic gravity potential for rigidly co-rotating observers,

$$U_{\text{Kerr}}^*/c^2 = -1 + \left(1 - \frac{2mr}{\rho(r, \vartheta)^2} + 4 \frac{\omega}{c} \frac{amr \sin^2 \vartheta}{\rho(r, \vartheta)^2} - \frac{\omega^2}{c^2} \sin^2 \vartheta \left(r^2 + a^2 + \frac{2mra^2 \sin^2 \vartheta}{\rho(r, \vartheta)^2} \right) \right)^{1/2}. \quad (54)$$

This potential can be used to compute redshifts, accelerations and the relativistic geoid in the Kerr spacetime. For $a \rightarrow 0$ the Schwarzschild result is recovered. Gravitomagnetic effects are included in two terms. One is proportional to $a\omega$ and the other is proportional to $a^2\omega^2$. The first term can change the sign depending on the direction of rotation.

IV. MAGNITUDES OF RELATIVISTIC EFFECTS ON THE GEOID

In this section, we determine and quantify the magnitudes of relativistic corrections to the Earth's geoid

at the leading order. We study a simple quadrupolar Earth model in the Newtonian theory and its relativistic generalization in the framework presented above. The best relativistic generalization of such a model is given by an appropriately constructed Erez-Rosen spacetime, see section III E 2. However, leading order effects are given by the first-order post-Newtonian approximation of the Erez-Rosen metric, which is the post-Newtonian metric constructed for a quadrupolar Newtonian potential according to Eq. (46).

The Earth's quadrupole moment¹⁴ $C_{20} \equiv J_2$, related to its flattening, gives the first (and by far the largest) non-trivial contribution to its gravitational field beyond the monopole. The quadrupole causes gravity to change from the equator towards the poles with a $\sin^2 \alpha$ like behavior, where α is the geocentric latitude. Hence, we expect relativistic corrections due to influence of the relativistic monopole and quadrupole (i) to induce an overall spherical correction due to the monopole and (ii) to yield latitude-dependent corrections about three orders of magnitude smaller since $J_2/J_0 \approx 10^{-3}$ for the Earth.

The methodology of this section is as follows. We use the Newtonian gravity potential (46) for a purely quadrupolar configuration and, thereupon, construct the post-Newtonian approximation of this situation to access the first-order relativistic contributions. Then, we construct the Newtonian geoid, based on the gravity potential W and the relativistic geoid based on our relativistic gravity potential U^* . In either case, we obtain a two-dimensional surface given by some function $x^1(x^2)$, where x^1 is a radial coordinate and x^2 is related to the polar angle.

The comparison of both results must be done in a way that eliminates coordinate ambiguities. We have decided to use an isometric embedding of the relativistic geoid surface into the three-dimensional Euclidean space \mathbb{R}^3 . If such an embedding is possible, it is unique and allows to investigate the intrinsic geometry of the relativistic geoid by applying well-known methods for the analysis of curved two-dimensional surfaces. The Newtonian geoid generically "lives" in this Euclidean space, and a comparison of closed two-dimensional surfaces in \mathbb{R}^3 is possible, e.g., in terms of their radial distance in any angular direction. Therefore, once the relativistic geoid is embedded, we can compare it to the Newtonian one and determine the difference. Note that such an embedding is in general only possible by numerical methods, even though the embedding equations can be given exactly, see the appendix for details.

However, we also have to overcome some subtle conventional issues. In the Newtonian case, the geoid is defined by the level surface of the gravity potential such that $|W| = W_0$ on its surface. Nowadays, W_0 is an agreed upon constant related to coordinate time transformations

¹³ Note that for this value the Kerr spacetime is actually over-extreme. However, this is true for any planet or star and horizons are of no interest since they are in the interior but the solution is valid and used for the exterior part only.

¹⁴ Note that both are positive in our convention, whereas in geodesy a different sign convention applies and $C_{20} \equiv -J_2$

from TCG to TAI scales, see Ref. [14]. Already in the Newtonian case, there are conceptual difficulties with properties of the geoid being “a mean sea surface fit” and the derived constant W_0 being not at all directly related to the sea surface. Let us, therefore, assume that some value W_0 is chosen, one way or another, that defines the Newtonian geoid. In the relativistic case, we define the geoid by one particular isochronometric surface, a level surface of the relativistic gravity potential U^* such that $U^*|_{\text{geoid}} = U_0^*$. Now, we need a clear prescription of how to choose the value U_0^* and how to relate it to W_0 . Hence, some gauge freedom is left in the choice of the constant. In the following, we consider different approaches and calculate the differences between the Newtonian and relativistic geoid in either case.

In approach (I), we choose $-U_0^* \equiv W_0$, which may be obvious regarding the Newtonian limit and is supported by the results of the previous section, as well as the proper time on the geoid and the defining constant L_g in the IAU resolution with its relation to W_0 .

In approach (II), we choose the value of U^* such that after the isometric embedding into \mathbb{R}^3 and comparison to the Newtonian geoid, the difference vanishes in the equatorial plane and is globally as small as possible. This means, we use the gauge freedom in the comparison such that the relativistic geoid is as close as possible to the Newtonian geoid.

In approach (III), we choose the value of U_0^* such that in its post-Newtonian expansion $W \rightarrow W_0$ and $U \rightarrow U_0$.

Finally, we also consider approach (IV), which is analogue to approach (I) but without embedding the relativistic geoid into \mathbb{R}^3 . Instead, we identify the global coordinates that are used for the Newtonian geoid and the relativistic post-Newtonian coordinates. This approach allows to judge whether or not the embedding is really necessary at the leading order or merely an academic endeavor.

A. Geoid models

The Newtonian gravity potential of a quadrupolar gravitational field is

$$W(R, \Theta) = -G \left(\frac{M}{R} + \frac{N_2 P_2(\cos \Theta)}{r^3} \right) - \frac{1}{2} R^2 \Omega^2 \sin^2 \Theta, \quad (55)$$

where $N_2 = J_2 R_\oplus^2 M_\oplus$. We use spherical coordinates (R, Θ, Φ) for the \mathbb{R}^3 , and R_\oplus , M_\oplus are the Earth’s radius and mass, respectively, and ω its angular velocity. The geoid as determined by observers on the rotating Earth, i.e. including centrifugal effects, in this model is the level surface of W such that

$$-W(R, \Theta)|_{\text{geoid}} = W_0 = 6.263\,685\,34 \times 10^7 \text{ m}^2 \text{ s}^{-2}. \quad (56)$$

For the post-Newtonian approximation of this configuration we have to use

$$\begin{aligned} U^*(r, \theta) &= U(r, \theta) - \frac{1}{2} r^2 \Omega^2 \sin^2 \theta + \frac{1}{2} \frac{U(r, \theta)^2}{c^2} \\ &= W(r, \theta) + \frac{1}{2} \frac{U(r, \theta)^2}{c^2}. \end{aligned} \quad (57)$$

The relativistic geoid is given by one chosen level surface of $U^*(r, \theta)$ such that

$$U^*(r, \theta)|_{\text{geoid}} = U_0^*. \quad (58)$$

We choose pseudo-spherical coordinates (r, θ, φ) for the post-Newtonian spacetime and the flat space coordinates (R, Θ, Φ) are their 0-th order approximations.

B. Geoid comparison approach (I)

Using the comparison method (I), we choose

$$U_0^* = -W_0 \quad (59)$$

and construct the relativistic geoid for the post-Newtonian configuration. The result is a two-surface described by $r(\theta)$. After embedding this surface into \mathbb{R}^3 , we determine the radial distance, at any polar angle, to the Newtonian geoid, which is generically given in \mathbb{R}^3 as a function $R(\Theta)$. The result is shown in Fig. 2. We find the mean difference between both geoids to be about 2 mm with some small angular deviations that are three orders of magnitude smaller due to the quadrupolar influence. Hence, we exactly find what we predicted at the beginning: the relativistic monopole causes a global deviation and the relativistic quadrupole induces some angular variation.

In a nutshell: the result is that the first order corrections to the Earth’s geoid due to General Relativity are about 2 mm with latitudinal variations of about $3 \mu\text{m}$.

C. Geoid comparison approach (II)

For the second approach, we choose the value U_0^* such that in the embedding space both geoids coincide in the equatorial plane. This choice can be easily translated into the structure of the embedding equations, see the appendix. However, in general it is not possible to deduce properties or parameter values in the spacetime from requirements which shall be fulfilled after an embedding. First, the equatorial radius R_0 of the Newtonian geoid is calculated and, thereupon, the solution $r_0(R_0)$ of $g_{\varphi\varphi}(r_0, \pi/2) = R_0^2$ is used as initial condition for the embedding equations, see Eq. (A11a). Thus, it is guaranteed that in the equatorial plane the embedded relativistic geoid has the same radius as the Newtonian one. In terms of the constant U_0^* this relates to the choice

$$\begin{aligned} U_0^* &= -W_0 - 0.02 \text{ m}^2 \text{ s}^{-2} \\ &= -6.263\,685\,34 \times 10^7 \text{ m}^2 \text{ s}^{-2} - 0.02 \text{ m}^2 \text{ s}^{-2}. \end{aligned} \quad (60)$$

Hence, there is a small difference between U_0^* and W_0 in this gauge, which is indeed below the contemporary accuracy of measurements for W_0 but corresponds to the next significant digit.

The result of this approach is shown in Fig. 3. We see that the overall modulation is almost completely removed, the mean value is about $4\ \mu\text{m}$, and only the latitudinal variation of about $8\ \mu\text{m}$ remains. By this choice, we have fitted the relativistic geoid to the Newtonian one in the best possible way and the influence of the relativistic monopole was reduced (or corrected for) as far as possible. The remaining difference is mainly due to the relativistic quadrupole. Hence, the freedom in the choice of gauge and convention can be used to minimize the differences between both geoids. Note that for this approach it is no longer true that $U_0^* = -W_0$ and the numerical values that define the surfaces of the relativistic and conventional geoid, respectively, are different, see above. No obvious a priori choice for the constant U_0^* can be made and this limits the geometric realization by measurement stations.

D. Geoid comparison approach (III)

For the third approach, we choose the value U_0^* such that

$$U_0^* = U^*|_{\text{geoid}} = U_{\text{pN}}^*|_{W \rightarrow -W_0, U \rightarrow U_0} = -W_0 + \frac{U_0^2}{2c^2}, \quad (61)$$

and the result is shown in Fig. 4. For this choice, the difference between Newtonian and relativistic geoid in the embedding space is about 4 mm with latitudinal variation of 0.02 mm between the poles and the equatorial plane. The disadvantage of this choice is that the value of U^* varies for each post-Newtonian order. Hence, we may exclude choices like the this from further analysis.

E. Geoid comparison approach (IV)

To emphasize the importance of the embedding, we compare the relativistic and Newtonian geoid also using approach (IV). The result is quite remarkable and shown in Fig. 5. We clearly see that, w.r.t. approach (I), the sign of the difference changes. As we can read off from Fig. 2 for approach (I), the radius of the relativistic geoid is globally about 2 mm larger than the radius of the Newtonian geoid. For approach (IV) it is vice versa! The “effect” appears due to the mismatch of the coordinates which is of the order of 4 mm at the involved distances such that pN radii are ‘smaller’ than Newtonian radii, in the sense of measuring true radial distances. Hence, the embedding is not only a theorists pedantism but really has an important influence on the result. It is, however, a mere coincidence that +2 mm become -2 mm by coordinate and embedding effects. Therefore statements on

the magnitude of “2 mm difference” between the geoids, as communicated in the geodetic community, remain correct; but signs do matter.

V. CONCLUSION AND OUTLOOK

We have shown how the definition of a relativistic gravitopotential leads to a definition of the relativistic geoid in analogy to the Newtonian understanding and expands the results that were presented in terms of the time-independent redshift potential in Ref. [12]. Our framework contains previously published results and generalizes Newtonian and post-Newtonian notions developed by other authors. The leading order difference of 2 mm between relativistic and conventional geoids might be detected with clocks and redshift measurements at the 10^{-19} level in the future. Therefore, clock networks using transportable optical clocks as well as clock stations and fiber networks can establish a realization of the relativistic geoid, see Refs. [4, 5, 34–39]. Moreover, our geoid definition can also be realized by acceleration measurements and determination of local plumb lines. For the realization of reference systems, the Global Geodetic Observing System (GGOS) of the International Association of Geodesy (IAG) demands 1 mm as accuracy and 0.1 mm/yr for its stability [40]. Thus, even today the relativistic geoid should be adopted in practice to fulfill these requirements and to be consistent with the relativistic treatment of the other geodetic methods (space geodetic techniques, reference frames, Earth rotation, etc.).

In follow-up publications we will focus on incorporating gravitomagnetic effects by expanding our results to spacetimes that allow to resemble the Earth’s monopole, quadrupole, and spin moments at the same time. Therefore, we need to overcome the limitation of the Kerr metric and use another class of spacetime models. Moreover, building on the present framework, we will generalize other geodetic notions such as the normal gravity field, height definitions for chronometric geodesy and relativistic leveling, and time scales as well as their relation to the proper time on the geoid.

ACKNOWLEDGEMENT

This work was supported by the Deutsche Forschungsgemeinschaft (DFG) through the Collaborative Research Center (SFB) 1128 geo-Q and the Research Training Group 1620 “Models of Gravity” as well as the Excellence Cluster “Quantum Frontiers” (EXC2123). We also acknowledge support by the German Space Agency DLR with funds provided by the Federal Ministry of Economics and Technology (BMWi) under Grant No. DLR 50WM1547 and the DLR institute for Satellite Geodesy and Inertial sensing. The authors would like to thank Volker Perlick, Dirk Puetzfeld, Heiner Denker, Domenico Giulini, and Sergei Kopeikin for helpful discussions.

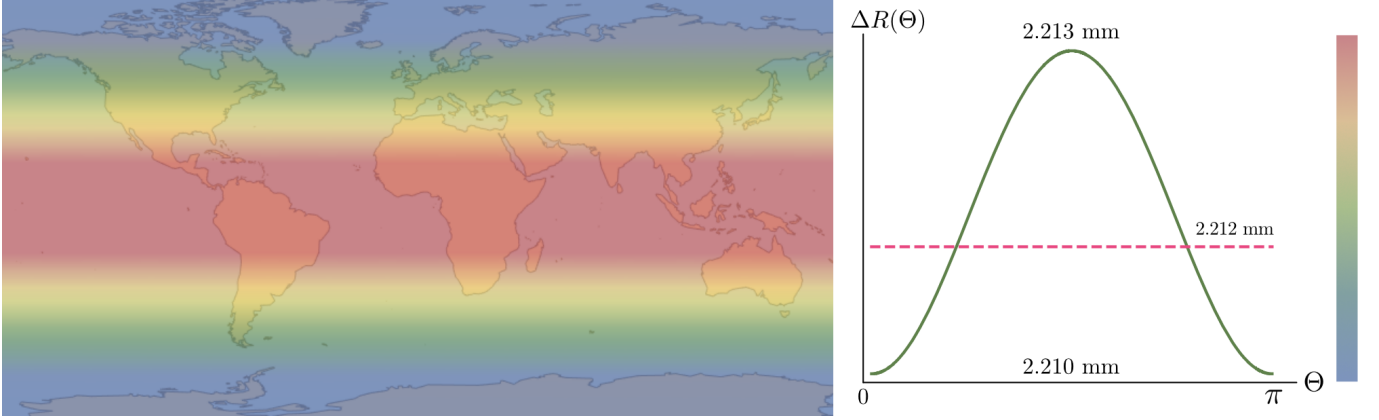


FIG. 2. Comparison of the relativistic and Newtonian geoid at leading order for approach (I). We show the geoid radii differences $\Delta R(\Theta) = R_{\text{PN}}(\Theta) - R_{\text{N}}(\Theta)$ in the embedding space \mathbb{R}^3 as a function of Θ . The maximal, minimal, and mean differences are indicated.

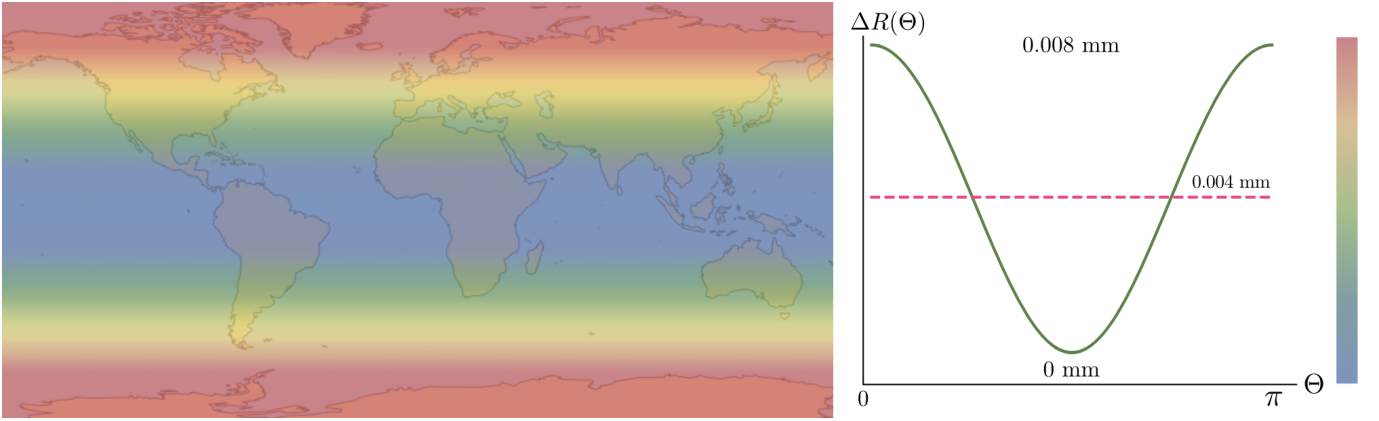


FIG. 3. Comparison of the relativistic and Newtonian geoid at leading order for approach (II). We show the geoid radii differences $\Delta R(\Theta) = R_{\text{PN}}(\Theta) - R_{\text{N}}(\Theta)$ in the embedding space \mathbb{R}^3 as a function of Θ . The maximal, minimal, and mean differences are indicated.

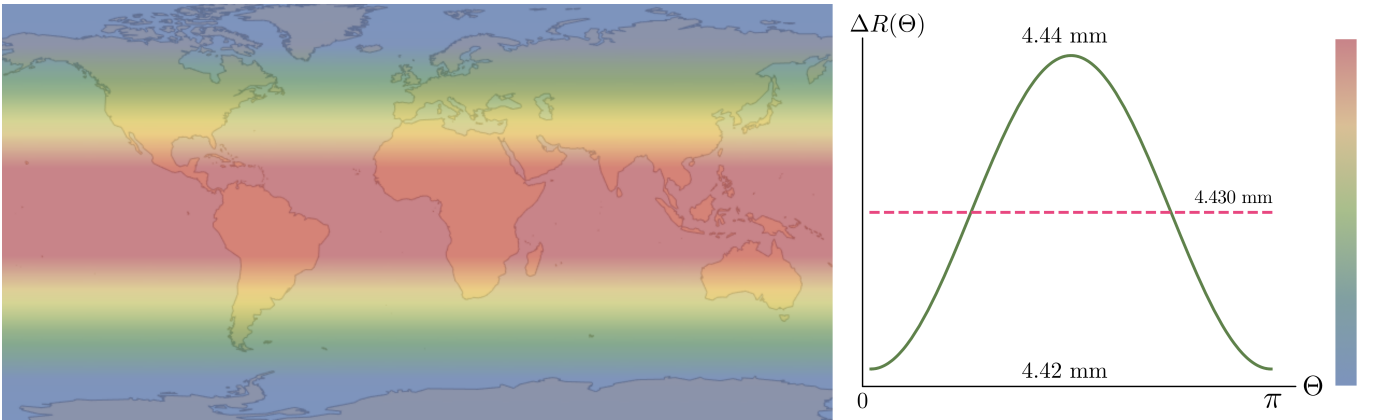


FIG. 4. Comparison of the relativistic and Newtonian geoid at leading order for approach (III). We show the geoid radii differences $\Delta R(\Theta) = R_{\text{PN}}(\Theta) - R_{\text{N}}(\Theta)$ in the embedding space \mathbb{R}^3 as a function of Θ . The maximal, minimal, and mean differences are indicated.

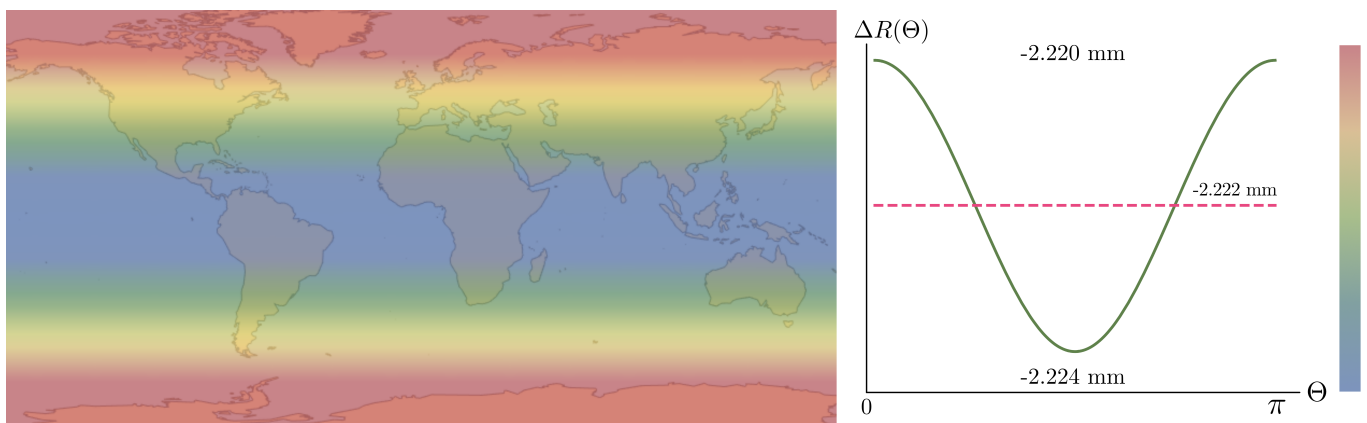


FIG. 5. Comparison of the relativistic and Newtonian geoid at leading order for approach (IV), which is the same as approach one but without embedding. We show the geoid radii differences $\Delta R(\Theta) = R_{\text{PN}}(\Theta) - R_{\text{N}}(\Theta)$, for which Newtonian and pN coordinates are identified, as a function of Θ . The maximal, minimal, and mean differences are indicated.

-
- [1] B. D. Tapley, S. Bettadpur, J. C. Ries, P. F. Thompson, and M. M. Watkins, *Science* **305**, 503 (2004).
- [2] B. D. Tapley, M. M. Watkins, F. Flechtner, C. Reigber, S. Bettadpur, M. Rodell, I. Sasgen, J. S. Famiglietti, F. W. Landerer, D. P. Chambers, J. T. Reager, A. S. Gardner, H. Save, E. R. Ivins, S. C. Swenson, C. Boening, C. Dahle, D. N. Wiese, H. Dobslaw, M. E. Tamisiea, and I. Velicogna, *Nature Climate Change* **9**, 358 (2019).
- [3] K. Abich, A. Abramovici, B. Amparan, A. Baatzsch, B. B. Okihiro, D. C. Barr, M. P. Bize, C. Bogan, C. Braxmaier, M. J. Burke, K. C. Clark, C. Dahl, K. Dahl, K. Danzmann, M. A. Davis, G. de Vine, J. A. Dickson, S. Dubovitsky, A. Eckardt, T. Ester, G. F. Barranco, R. Flatscher, F. Flechtner, W. M. Folkner, S. Francis, M. S. Gilbert, F. Gilles, M. Gohlke, N. Grossard, B. Guenther, P. Hager, J. Hauden, F. Heine, G. Heinzl, M. Herding, M. Hinz, J. Howell, M. Katsumura, M. Kaufer, W. Klipstein, A. Koch, M. Kruger, K. Larsen, A. Lebeda, A. Lebeda, T. Leikert, C. C. Liebe, J. Liu, L. Lobmeyer, C. Mahrtdt, T. Mangoldt, K. McKenzie, M. Misfeldt, P. R. Morton, V. Müller, A. T. Murray, D. J. Nguyen, K. Nicklaus, R. Pierce, J. A. Ravich, G. Reavis, J. Reiche, J. Sanjuan, D. Schütze, C. Seiter, D. Shaddock, B. Sheard, M. Sileo, R. Spero, G. Spiers, G. Stede, M. Stephens, A. Sutton, J. Trinh, K. Voss, D. Wang, R. T. Wang, B. Ware, H. Wegener, S. Windisch, C. Woodruff, B. Zender, and M. Zimmermann, *Phys. Rev. Lett.* **123**, 031101 (2019).
- [4] T. Takano, M. Takamoto, I. Ushijima, N. Ohmae, T. Akatsuka, A. Yamaguchi, Y. Kuroishi, H. Munekane, B. Miyahara, and H. Katori, *Nature Photonics* **10**, 662 (2016).
- [5] J. Müller, D. Dirckx, S. M. Kopeikin, G. Lion, I. Panet, G. Petit, and P. N. A. M. Visser, *Space Science Reviews* **214**, 5 (2017).
- [6] S. M. Kopeikin, V. F. Kanushin, A. P. Karpik, A. S. Tolstikov, E. G. Gienko, D. N. Goldobin, N. S. Kosarev, I. G. Ganagina, E. M. Mazurova, A. A. Karaush, and E. A. Hanikova, *Gravitation and Cosmology* **22**, 234 (2016).
- [7] P. Delva, H. Denker, and G. Lion, in *Relativistic Geodesy: Foundations and Applications* (Springer, to appear 2018).
- [8] C. M. Will, *Living Reviews in Relativity* **17**, 4 (2014).
- [9] A. Bjerhammar, *Bull. Géodésique* **59**, 207 (1985).
- [10] A. Bjerhammar, *Relativistic Geodesy*, Tech. Rep. NOS 118 NGS 36 (1986).
- [11] M. H. Soffel, H. Herold, H. Ruder, and M. Schneider, *Manuscripta Geodaetica* **13**, 143 (1988).
- [12] D. Philipp, V. Perlick, D. Puetzfeld, E. Hackmann, and C. Lämmerzahl, *Phys. Rev. D* **95**, 104037 (2017).
- [13] W. Torge and J. Müller, *Geodesy* (De Gruyter, Berlin, 2012).
- [14] L. Sánchez, R. Čunderlík, N. Dayoub, K. Mikula, Z. Minarechová, Z. Šíma, V. Vatrt, and M. Vojtíšková, *Journal of Geodesy* **90**, 815 (2016).
- [15] D. Philipp, V. Perlick, D. Puetzfeld, E. Hackmann, and C. Lämmerzahl, in *2017 IEEE International Workshop on Metrology for AeroSpace (MetroAeroSpace)* (2017) pp. 114–119.
- [16] D. Philipp, *Theoretical Aspects of Relativistic Geodesy*, Ph.D. thesis, University of Bremen, Germany (2018).
- [17] S. M. Kopeikin, *Manuscr. Geod.* **16** (1991).
- [18] S. M. Kopeikin, *AIP Conference Proceedings* **886**, 268 (2007).
- [19] S. M. Kopeikin, E. M. Mazurova, and A. P. Karpik, *Phys. Lett. A* **379**, 1555 (2015).
- [20] M. Oltean, R. J. Epp, P. L. McGrath, and R. B. Mann, *Classical Quantum Grav.* **33** (2016).
- [21] D. Puetzfeld, Y. N. Obukhov, and C. Lämmerzahl, *Phys. Rev. D* **98**, 024032 (2018).
- [22] M. Soffel and F. Frutos, *J. Geod.* **90**, 1345 (2016).
- [23] M. H. Soffel, *Relativity in Astrometry, Celestial Mechanics and Geodesy*, Astronomy and Astrophysics Library (Springer, Berlin Heidelberg, 1989).
- [24] S. M. Kopeikin, M. Efroimsky, and G. Kaplan, *Relativistic Celestial Mechanics of the Solar System* (Wiley-VCH, Weinheim, Germany, 2011).
- [25] E. Poisson and C. M. Will, *Gravity: Newtonian, Post-Newtonian, Relativistic* (Cambridge University Press, 2014).
- [26] C. M. Will, *Theory and Experiment in Gravitational Physics* (Cambridge University Press, 1993).
- [27] H. Quevedo, *Phys. Rev. D* **39**, 2904 (1989).
- [28] G. Erez and N. Rosen, *Bull. Res. Coun. Isr.* **8F**, 47 (1959).
- [29] H. Stephani, D. Kramer, M. MacCallum, C. Hoenselaers, and E. Herlt, *Exact Solutions of Einstein's Field Equations*, 2nd ed. (Cambridge University Press, Cambridge, England, 2003).
- [30] H. Bateman and A. Erdélyi, *Higher Transcendental Functions*, Higher Transcendental Functions, Vol. 1 (McGraw-Hill, New York, 1955).
- [31] R. P. Geroch, *J. Math. Phys.* **11**, 2580 (1970).
- [32] R. O. Hansen, *J. Math. Phys.* **15**, 46 (1974).
- [33] F. Lemoine, S. Kenyon, J. Factor, R. Trimmer, N. Pavlis, D. Chinn, C. Cox, S. Klosko, S. Luthcke, M. Torrence, Y. Wang, R. Williamson, E. Pavlis, R. Rapp, and T. Olson, *The development of the joint NASA GSFC and the National Imagery and Mapping Agency (NIMA) Geopotential Model EGM96* (National Aeronautics and Space Administration, Goddard Space Flight Center, 1998) p. 575 p. in various pagings .
- [34] S. Droste, F. Ozimek, T. Udem, K. Predehl, T. W. Hänsch, H. Schnatz, G. Grosche, and R. Holzwarth, *Phys. Rev. Lett.* **111**, 110801 (2013).
- [35] C. Lisdat, G. Grosche, N. Quintin, C. Shi, S. M. F. Raupach, C. Grebing, D. Nicolodi, F. Stefani, A. Al-Masoudi, S. Dörscher, S. Häfner, J.-L. Robyr, N. Chiodo, S. Bilicki, E. Bookjans, A. Koczwarra, S. Koke, A. Kuhl, F. Wiotte, F. Meynadier, E. Camisard, M. Abgrall, M. Lours, T. Legero, H. Schnatz, U. Sterr, H. Denker, C. Chardonnet, Y. Le Coq, G. Santarelli, A. Amy-Klein, R. Le Targat, J. Lodewyck, O. Lopez, and P.-E. Pottie, *Nature Communications* **7**, 12443 (2016).
- [36] J. Guéna, S. Weyers, M. Abgrall, C. Grebing, V. Gerginov, P. Rosenbusch, S. Bize, B. Lipphardt, H. Denker, N. Quintin, S. Raupach, D. Nicolodi, F. Stefani, N. Chiodo, S. Koke, A. Kuhl, F. Wiotte, F. Meynadier, W. Camisard, E. Chardonnet, Y. Le Coq, M. Lours, G. Santarelli, A. Amy-Klein, R. Le Targat, O. Lopez, P. E. Pottie, and G. Grosche, *Metrologia* **54**, 348 (2017).

- [37] P. Delva, J. Lodewyck, S. Bilicki, E. Bookjans, G. Vallet, R. Le Targat, P.-E. Pottie, C. Guerlin, F. Meynadier, C. Le Poncin-Lafitte, O. Lopez, A. Amy-Klein, W.-K. Lee, N. Quintin, C. Lisdat, A. Al-Masoudi, S. Dörscher, C. Grebing, G. Grosche, A. Kuhl, S. Raupach, U. Sterr, I. R. Hill, R. Hobson, W. Bowden, J. Kronjäger, G. Marra, A. Rolland, F. N. Baynes, H. S. Margolis, and P. Gill, *Phys. Rev. Lett.* **118**, 221102 (2017).
- [38] J. Grotti, S. Koller, S. Vogt, S. Häfner, U. Sterr, C. Lisdat, H. Denker, C. Voigt, L. Timmen, A. Rolland, F. N. Baynes, H. S. Margolis, M. Zampaolo, P. Thoumany, M. Pizzocaro, B. Rauf, F. Bregolin, A. Tampellini, P. Barbieri, M. Zucco, G. A. Costanzo, C. Clivati, F. Levi, and D. Calonico, *Nature Physics* **14**, 437 (2018).
- [39] T. E. Mehlstäubler, G. Grosche, C. Lisdat, P. O. Schmidt, and H. Denker, *Reports on Progress in Physics* **81**, 064401 (2018).
- [40] H.-P. Plag and M. Pearlman, eds., *Global Geodetic Observing System* (Springer Berlin Heidelberg, 2009).

Appendix A: Isometric Embedding into Euclidean Space

To investigate and visualize the intrinsic geometry of the relativistic geoid, which is described by a particular isochronometric surface, i.e. a level surface of the relativistic gravity potential $U^*|_{\text{geoid}} = U_0^* = \text{const.}$, we isometrically embed this surface into Euclidean space \mathbb{R}^3 . If such an embedding is possible, the embedded surface shows the intrinsic geometry of the geoid.

In all our axisymmetric models, the relativistic geoid is a level surface

$$U^*(x, y)|_{\text{geoid}} = U_0^* = \text{const.}, \quad (\text{A1})$$

where x and y are the two spatial coordinates, related to a radius measure and the polar angle, respectively.

For any such two-dimensional surface defined by Eq. (A1), the following is true everywhere on the surface

$$0 = dU^* = \partial_x U^*(x, y) dx + \partial_y U^*(x, y) dy. \quad (\text{A2})$$

Hence, we have on the geoid surface

$$dx = - \left(\frac{\partial_y U^*(x, y)}{\partial_x U^*(x, y)} \right) dy, \quad (\text{A3})$$

which yields a relation $x = x(y)$ that describes this surface.

On the surface $U^*(x, y) = U_0^*$ there is a two-dimensional Riemannian metric defined according to

$$g^{(2)} = (g_{xx}(x, y) x'(y)^2 + g_{yy}(x, y)) dy^2 + g_{\varphi\varphi}(x, y) d\varphi^2, \quad (\text{A4})$$

where φ is the azimuthal angle related to the axisymmetry of the spacetime model.

We want to isometrically embed the surface $U^*(x, y) = U_0^*$ into Euclidean 3-space \mathbb{R}^3 with cylindrical coordinates

(Λ, φ, Z) , where Z is the height, Λ is the radius in the $Z = 0$ plane, and φ is the azimuthal angle. The Riemannian metric in \mathbb{R}^3 can then be written as

$$g_E^{(3)} = dZ^2 + d\Lambda^2 + \Lambda^2 d\varphi^2. \quad (\text{A5})$$

The two embedding functions $Z(y)$ and $\Lambda(y)$ can now be determined from

$$[g_{xx}(x(y), y) x'(y)^2 + g_{yy}(x(y), y)] dy^2 + g_{\varphi\varphi}(x(y), y) d\varphi^2 \quad (\text{A6})$$

$$= (Z'(y)^2 + \Lambda'(y)^2) dy^2 + \Lambda^2(y) d\varphi^2. \quad (\text{A7})$$

If Eq. (A3) allows an explicit solution for $x = x(y)$, the result is inserted into (A6). A comparison of coefficients leads to

$$\Lambda(y) = \sqrt{g_{\varphi\varphi}(x, y)} \Big|_{x=x(y)}, \quad (\text{A8a})$$

$$Z(y) = \pm \int_0^y dy \left(g_{xx}(x, y) \left(\frac{\partial_y U^*(x, y)}{\partial_x U^*(x, y)} \right)^2 + g_{yy}(x, y) - \frac{g'_{\varphi\varphi}(x, y)^2}{4g_{\varphi\varphi}(x, y)} \right)^{1/2} \Big|_{x=x(y)}. \quad (\text{A8b})$$

Here, $g'_{\varphi\varphi}$ means that $x(y)$ is inserted first and then the derivative w.r.t. y is taken. In general, Eq. (A8b) can only be integrated numerically.

The solutions of Eqs. (A8a) and (A8b) yield the cylindrical radius coordinate Λ and the height Z in \mathbb{R}^3 as functions of $y \in [-1, 1]$. This corresponds to a polar angle $\vartheta \in [0, \pi]$. Using the height and radius functions, a section of the embedded surface is obtained. Due to the axi-symmetry, the full embedded surface is obtained by a rotation of this section. For all values of y for which it is true that

$$g_{xx}(x, y) \left(\frac{\partial_y U^*(x, y)}{\partial_x U^*(x, y)} \right)^2 + g_{yy}(x, y) > \frac{g'_{\varphi\varphi}(x, y)^2}{4g_{\varphi\varphi}(x, y)}, \quad (\text{A9})$$

the embedding is possible. If the embedding into \mathbb{R}^3 is not possible, different means of visualization and comparison of the relativistic geoid must be employed.

If Eq. (A3) can not be solved for $x = x(y)$, we have to use Eq. (A2), which leads to

$$x'(y) = \frac{dx}{dy} = - \frac{\partial_y U^*(x, y)}{\partial_x U^*(x, y)}. \quad (\text{A10})$$

Together with Eqs. (A8a) and (A8b) the following coupled system of differential equations must be solved

$$x'(y) = - \frac{\partial_y U^*(x, y)}{\partial_x U^*(x, y)} \Big|_{x=x(y)}, \quad (\text{A11a})$$

$$\Lambda(y) = \sqrt{g_{\varphi\varphi}(x(y), y)}, \quad (\text{A11b})$$

$$Z'(y) = \pm \sqrt{g_{xx}(x(y), y) (x'(y))^2 + g_{yy}(x(y), y) - \Lambda'(y)^2}. \quad (\text{A11c})$$

The initial conditions can be given in the equatorial plane ($y = 0$) such that $x(0) = x_0$, $Z(0) = 0$.

Appendix B: Legendre functions of the second kind

In the following we list the first few Legendre functions of the second kind Q_l which appear in the present work for the sake of clarity. We refer to, e.g., Ref. [30] for details.

The first four functions are

$$Q_0(x) = \frac{1}{2} \log \frac{x-1}{x+1}, \quad (\text{B1a})$$

$$Q_1(x) = \frac{1}{2} x \log \frac{x-1}{x+1} - 1, \quad (\text{B1b})$$

$$Q_2(x) = \frac{1}{2} P_2(x) \log \frac{x-1}{x+1} - \frac{3}{2} x, \quad (\text{B1c})$$

$$Q_3(x) = \frac{1}{2} P_3(x) \log \frac{x-1}{x+1} - \frac{5}{2} x^2 + \frac{2}{3}, \quad (\text{B1d})$$

and the general structure is

$$Q_l(x) = \frac{1}{2} P_l(x) \log \frac{x-1}{x+1} + \mathcal{P}_{l-1}(x), \quad (\text{B2})$$

where $\mathcal{P}_{l-1}(x)$ is a polynomial of degree $l-1$.